ORIGINAL RESEARCH

Slow release curcumin-containing soy protein nanoparticles as anticancer agents for osteosarcoma: synthesis and characterization

Hadi Zare-Zardini[1,2,3] · Hossein Soltaninejad[4] · Adel Ghorani-Azam[5] · Reza Nafisi-Moghadam[6] · Navid Haddadzadegan[7] · Mojtaba Ansari[2] · Seyed Houssein Saeed-Banadaki[8] · Mohammad Reza Sobhan[8] · Sima Mozafari[2] · Mahlagha Zahedi[9]

Abstract

Curcumin-containing soy protein nanoparticles (curcumin–SPNs) were synthesized by desolvation (coacervation) method and characterized by SEM, DLS, FTIR, and XRD. For anticancer evaluation, osteogenic sarcoma (SAOS2) cell lines were incubated with different concentrations of nanostructures. The dialysis method was used for assessment of drug release. Intracellular reactive oxygen species (ROS) were evaluated in IC50 dose after 24 h of exposure to free curcumin and curcumin–SPNs. Characterization data showed that the size of drug-free SPNs and curcumin–SPNs were 278.2 and 294.7 nm, respectively. The zeta potential of drug-free SPNs and curcumin–SPNs were -37.1 and -36.51 mv, respectively. There was no significant difference between the control and drug-free SPNs groups in terms of cell viability ($p > 0.05$). The viability of cells in different concentrations of the designed curcumin–SPNs in Saos2 cell line was significantly higher than free drug ($p < 0.05$). The release of curcumin showed that more than 50% of the drug was released in the first 2 h of incubation. After this time, the slow release of drug was continued to 62–83% of drug. IC50 values of free curcumin and curcumin–SPNs (1/10) were 156.8 and 65.9 μg/mL, respectively (a free curcumin IC50 was 2.4 times more than curcumin–SPNs). Slow-release of the curcumin causes the cell to be exposed to the anticancer drug for a longer period of time. The intracellular ROS levels significantly increased in an IC50 dose after 24 h of exposure to both free curcumin and curcumin–SPNs compared with controls ($p < 0.05$).

Keywords Curcumin · Soy protein · Nanoparticle · Saos2 cell lines

Introduction

Osteosarcoma is considered as the main malignancy of the bone (Corre et al. 2020). The prevalence of this type of bone tumor is 30–45% (Jafari et al. 2020). Pulmonary metastases and rapid tumor development are the main causes of mortality in patients with osteosarcoma (Xin and Wei 2020), and the mortality rate of this disease is 90% (Hashimoto et al. 2020). Dysfunction of the bone also occurs in osteosarcoma due to bone metastases. Similar to other cancer, surgery and

✉ Hadi Zare-Zardini
  hadizarezardini@gmail.com

1 Department of Biomedical Engineering, Meybod University, Meybod, Iran

2 Hematology and Oncology Research Center, Shahid Sadoughi University of Medical Sciences, Yazd, Iran

3 Medical Nanotechnology and Tissue Engineering Research Center, Yazd Reproductive Sciences Institute, Shahid Sadoughi Hospital, Shahid Sadoughi University of Medical Sciences, Yazd, Iran

4 Faculty of Interdisciplinary Science and Technology, Tarbiat Modares University, Tehran, Iran

5 Department of Forensic Medicine and Toxicology, School of Medicine, Urmia University of Medical Sciences, Urmia, Iran

6 Department of Radiology, Shahid Sadoughi University of Medical Sciences, Yazd, Iran

7 Department of Anesthesiology and Critical Care, Shahid Sadoughi University of Medical Sciences, Yazd, Iran

8 Department of Orthopedia, Shahid Sadoughi University of Medical Sciences, Yazd, Iran

9 Department of Pathology, Shahid Sadoughi University of Medical Sciences, Yazd, Iran

chemotherapy are the two main treatment approaches for osteosarcoma (Durfee et al. 2016), while this type of tumor is resistant to radiotherapy. On the other hand, the success rate of chemotherapy is not complete (Zhao et al. 2021). Therefore, the development of new therapeutic strategies is necessary. Medicinal plants have numerous biologically active components that can be used in various medical applications such as treatment of various types of diseases including cancers http://doi.org/10.1002/ptr.6120, http://doi.org/10.1093/chromsci/bmaa108. Accordingly, medicinal plants can be used to develop new pharmacologically active agents for reduction of mortality and the side effects of osteosarcoma (Ege and Yumrutas 2020; Mokaramat-Yazdi et al. 2021; Mokarramat-Yazdi et al. 2020; Mpingirika et al. 2020). Curcumin (1,7-bis(4-hydroxy-3-methoxyphenyl)-1,6-heptadiene-3,5-dione) is a natural product originated from *Curcuma longa* species (Hewlings and Kalman 2017). This natural polyphenol has three reactive sites: metal chelator, Michael acceptor, and hydrogen atom donor (Mansouri et al. 2020). These reactive groups are the key elements and responsible for curcumin stability in treatment of diseases such as inflammation, oxidative stress, cancer, etc. (Mansouri et al. 2020). Tumor suppression is one of the most important biological activity of curcumin (Weng and Goel 2020). This agent is commercially produced as anticancer drug. Based on literature review, curcumin has potent anticancer activities against osteosarcoma through apoptosis induction and inhibition/induction of various agents such as cytokines, growth factors, and enzymes (cyclooxygenase II (COX-2), protein kinase D1 (PKD1)) (Elamin et al. 2021; Kabir et al. 2021; Mortezaee et al. 2019; Semlali et al. 2021). On the other hand, curcumin can recover the related bone defects owing to tumor erosion or surgery (Giordano and Tommonaro 2019; Weng and Goel 2020). Low aqueous solubility and fast decomposition (low bioavailability) can lead to reduction of chemical stability, oral bioavailability, and cellular uptake, which limit the biological applications of curcumin (Stanić 2017). Thus, improvement of the above mentioned limitations can enhance the anticancer efficacy of curcumin. In between, nanostructures can provide these favorable conditions (Alemi et al. 2018; Zare-Zardini et al. 2020). Protein nanoparticles, especially soy proteins nanoparticles (SPNs), are novel structures for encapsulation and delivery of bioactive molecules and drugs (Hong et al. 2020; Riahi-Zanjani et al. 2019). SPNs are commonly synthesized by controlled partial enzymatic hydrolysis. These synthesized nanoparticles, as one of the most abundant protein nanoparticles, are widely used for nutraceutical and drug encapsulation (Wang et al. 2020). These natural nanostructures can improve the therapeutic index of therapeutic agents, such as curcumin, by changing drug absorption, reducing metabolism, prolonging half-life, and minimizing the toxicity (Verma et al. 2018). Findings have shown that these nanostructures can be used as delivery systems for various natural and synthetic drugs (Mohseni et al. 2014). Different nanostructures have been used for curcumin delivery such as nanogels, nanodisks, micelles, solid lipid nanoparticles, liposome, gold nanoparticles, magnetic nanoparticles, and polymers. Enhancement of solubility and bioavailability and reduction of hydrolysis and inactivation are the main reason for application of these nanostructures (Anitha et al. 2014; Basnet et al. 2012; Bhandari et al. 2016; Chaurasia et al. 2016; Kakkar et al. 2011; Nambiar et al. 2018; Ntoutoume et al. 2016; Tefas et al. 2017; Vetha et al. 2019). Teng et al. (2012) used soy protein nanoparticles for slow release of curcumin. We used a similar procedure for nanoparticle preparation with proper modification. For this purpose, we used different concentration of curcumin as well as different ratios of curcumin/nanoparticles. Also, we evaluated the anticancer activity of the designed nanostructures on osteosarcoma. There is no similar study with all the mentioned methods. Hence, in this study, curcumin-containing soy protein nanoparticles was synthesized, characterized, and used as anticancer agent for the treatment of osteosarcoma.

Materials and methods

Materials

Osteogenic sarcoma (SAOS2) cell line was purchased from Pasteur Institute (Tehran, Iran). Culture medium (Dulbecco's modified Eagle medium with high glucose), fetal bovine serum (FBS), trypsin/EDTA, and penicillin/streptomycin were purchased from Gibco (Scotland). Other materials, such as curcumin, phosphate buffered saline (PBS), glutaraldehyde, ethanol, 3(4,5-dimethlthiazol-2-yl)-2,5-diphenyltetrazolium bromide (MTT), *tert*-butyl hydroperoxide, and dimethyl sulfoxide (DMSO) were purchased from Sigma–Aldrich (Germany).

Nanoparticle synthesis

Soy protein contents were achieved by salt precipitation through ammonium sulphate gradient. Desolvation method was used for preparation of SPNs. Briefly, 1.5 g of acquired soy protein isolates from solution salt precipitation were desalinated and diluted by ethanol with final concentration of 4.5 mg/mL. This solution was incubated for 15 min. After this time, glutaraldehyde (20 mg/mL) was diluted by adding 50 mL ethanol. Then, rotary evaporation was used to remove the ethanol. Ethanol was replaced with the same volume of deionized water. The acquired solution was centrifuged for 20 min. The supernatant was stored at 4 °C.

Curcumin loading

For preparation of curcumin–SPNs, ethanolic solution of curcumin (5 mg/mL) was added to aquatic solution of soy protein contents (50 mg/mL) with different ratios (curcumin/SPNs: 1/10, 1/20, 1/30, and 1/40). These acquired solutions were cross-linked by glutaraldehyde. The prepared structures were diluted and centrifuged, and the acquired supernatants were stored at 4 °C.

Characterization of nanoparticles

Characterization of the produced nanoparticle was performed by Dynamic Laser Scattering (DLS), Fourier-transform infrared spectroscopy (FTIR), X-ray diffraction (XRD), and Scanning Electron Microscopy (SEM). DLS was used for the determination of size distribution and charge. DLA was performed by Count Particle Laser instrument of 637 nm and a scattering angle of 90°. Analysis was performed for 1 min at 25 °C. For accurate functionalization, FTIR technique was applied. For this purpose, acquired nanostructures were lyophilized, and 1 mg of the powder of each sample was mixed with 100 mg of potassium bromide powder and pressed as a tablet. Each tablet was analyzed by FTIR in wavenumber range of 400–4000 cm^{-1} at a resolution of 4 cm^{-1}. SEM was used to determine the surface topology. A drop of nanoparticle colloidal solution was placed on a slide and after drying at room temperature, it was covered with gold powder and placed in an SEM device and photographed. XRD was also used for identification of the crystalline mineralogical phases of the powders. Debye–Scherrer formula for crystallite size determination is given by the following equation:

$$D = \frac{0.94\lambda}{\beta\cos\theta}, \tag{1}$$

where D: crystallite size, λ: wavelength of X-ray, β: full width at half maximum, and θ: Bragg's angle (Soltaninejad et al. 2020, 2021).

Determination of encapsulation efficiency and release evaluation

A standard curve was prepared by different concentrations of curcumin and absorbance at 426 nm. The method of approach studied by Natale et al. was used for determination of encapsulation efficiency with modification (Di Natale et al. 2020). In this method, solution containing curcumin–SPNs and free curcumin was centrifuged and supernatant was collected. The precipitation was dissolved in 10 mL of ethanol for 5 min. After this time, the solution was centrifuged for precipitation of protein section. The supernatant was analyzed by UV/Vis spectrophotometer at 426 nm. The absorbance result was changed to concentrations by the above standard curve. This acquired concentration belongs to loaded drugs into SPNs.

Encapsulation efficacy (EE) was calculated by the following equation:

$$EE\ (\%) = [(entrapped\ drug)/drug\ added]. \tag{2}$$

The release of curcumin from SPNs was evaluated by dialysis method at 37 °C and pH 7.4. For calculation of the released drug, the dialysis medium was replaced at different times immediately with the same volume of fresh PBS. The absorbance of samples was read using spectrophotometers at 426 nm.

Anticancer activity evaluation

Human bone cell line (Saos2) was used for anticancer activity evaluation. After cell culture, the cells were treated with different concentrations of the prepared nanostructures for 24, 48, and 72 h. At the end, the treated cells were washed with PBS and mixed with diluted MTT for 4 h to form formazan crystal. Internal solution of each well was removed and dimethyl sulfoxide (DMSO) (200 μL) was added. The absorbance of samples was measured at 570 nm and the cell viability was calculated via Eq. (3):

$$Viable\ cells(\%) = \frac{Mean\ optical\ absorption\ in\ test\ group - Average\ light\ absorption\ in\ culture\ medium}{Mean\ optical\ absorption\ in\ control\ group - Average\ light\ absorption\ in\ culture\ medium}. \tag{3}$$

Graph pad software was sued for calculation of IC50.

Reactive oxygen species

For evaluation of intracellular reactive oxygen species (ROS), the treated cells were obtained and washed by PBS solution. Basal and induced intracellular ROS levels were assessed in the absence and presence of the standard inducer of ROS production *tert*-butyl hydroperoxide (TBHP; I36007; molecular probes).

An oxidation-sensitive fluorescent probe, 5-(and-6)-carboxy-2′,7′-dichloro-dihydrofluorescein diacetate (carboxy-H2DCFDA; I36007; molecular probes) was used for assessment of ROS concentration. Based on Kim et al. study (Kim et al. 2013), the preparation and incubation protocol applied for all treated and control cell lines. All samples were centrifuged at 1.5 rpm for 5 min following incubation and washing with PBS buffer. Finally, 500 µL staining buffer plus cell suspension was observed using Facscalibur flow cytometer system (Becton Dickinson Biosciences, CA, USA). The data were analyzed by FlowJo software (version 10.4).

Results

Characterization results

The result of FTIR analysis is summarized in Fig. 1. According to this figure, SPNs and curcumin–SPNs had similar spectroscopic pattern with observable peaks at 1630–1640 (C–O stretching vibration), 1530–1540 (NH bending vibration of amide II), 1450–1460 (COOH stretching vibration), and 1230–1240 (C–H bending vibration). Curcumin was
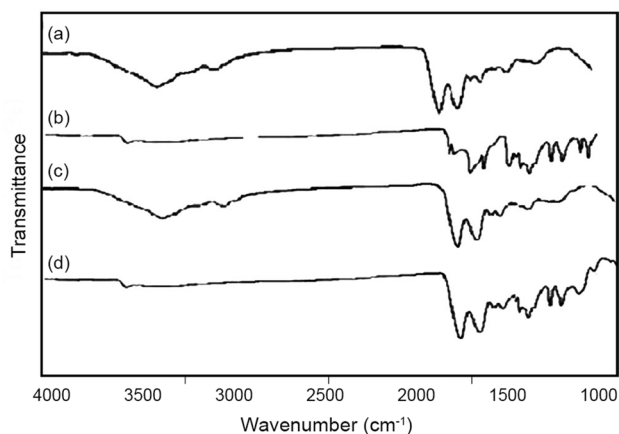

Fig. 1 FTIR spectra of designed nanostructures. **A** SPNs, **B** curcumin, **C** curcumin–SPNs, and **D** physical mix of curcumin and SPNs
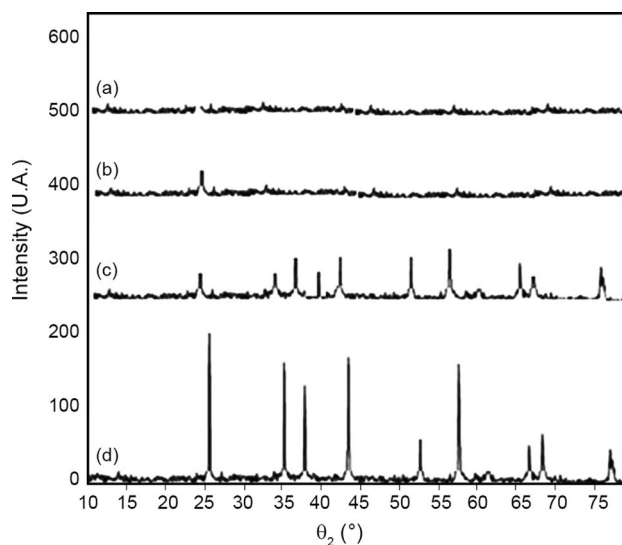

Fig. 2 XRD patterns of designed nanostructures. **A** SPNs, **B** curcumin–SPNs, **C** physical mix of curcumin and SPNs and **D** curcumin

characterized by two main peaks at 1103 (C–O–C stretching vibration), and 1419 (C–OH stretching vibration). In physical mixture of SPNs and curcumin, there are observable peaks as: 1630–1640 (C–O stretching vibration), 1530–1540 (NH bending vibration of amide II), 1450–1460 (COOH stretching vibration), 1630–1640 (C–O stretching vibration), 1103 (C–O–C stretching vibration), and 1419 (C–OH stretching vibration). In FTIR spectra of curcumin–SPNs, the indicator peaks at 1630–1640 (C–O stretching vibration), 1530–1540 (NH bending vibration of amide II), 1450–1460 (COOH stretching vibration), and 1230–1240 (C–H bending vibration) were observable.

Figure 2 shows the XRD pattern of curcumin and the prepared nanostructures. In the XRD pattern of curcumin, the characteristic peaks indicated its potent crystalline nature. These peaks are observable with lower intensity in the XRD pattern of physical mixture of SPNs and curcumin. In the XRD pattern of SPNs and curcumin–SPNs, there are no characteristic peaks due to encapsulation of curcumin in SPNs.

Table 1 The efficiency of curcumin entrapment efficiency, size, and zeta potential in different formulation of curcumin–SPNs

Curcumin/SPNs	Size	Zeta potential	Entrapment efficiency (%)
SPNs	278.2	− 37.1	–
1/10	294.7	− 36.51	82.8
1/20	321.84	− 35.85	75.2
1/30	362.4	− 34.14	74.1
1/40	392.8	− 33.75	48.4

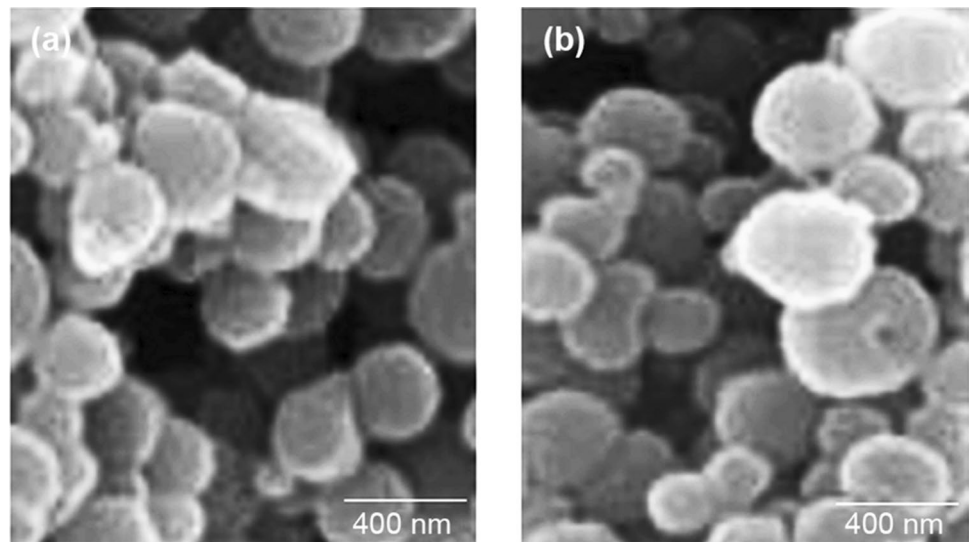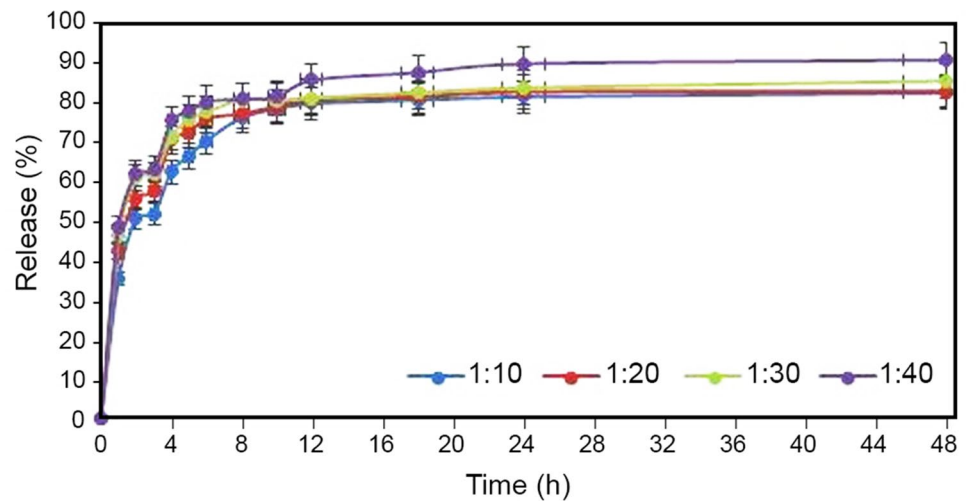**Fig. 3** SEM images of SPNs (**A**) and curcumin–SPNs (**B**)

Fig. 4 Drug release in different ratio of curcumin/SPNs (1:10, 1:20, 1:30, and 1:40)

The size and zeta potential were 321.84 nm and -31.85 for curcumin–SPNs under the best drug loading conditions (Table 1).

SEM images also showed similar data. Based on Fig. 3, size and shape of SPNs and curcumin–SPNs are compatible with other characterization data.

Investigation of drug loading and release

The efficiency of curcumin loading in different concentrations of SPNs is summarized in Table 1. Based on this table, drug loading was successfully done in all situations. The best drug entrapment efficiency occurred in 1/10 of curcumin/SPNs (82.8%).

Figure 4 indicates that at the same time, the ratio of 1/40 curcumin/SPNs had the highest drug release percentage in comparison with other ratios. In this ratio, the release of curcumin under physiological conditions (temperature of 37 °C

and a pH of 7.4) indicated that in the first 2 h, more than 50% of the drug was released. After this time, slow drug release was occurred. The maximum drug release during 48 h was 81.6, 82.1, 84.6, and 89.9% for the ratio of 1/10, 1/20, 1/30, and 1/40 curcumin/SPNs, respectively.

Anticancer activity

Evaluation of toxicity of drug-free SPNs showed that this nanostructure had no toxicity on SAOS2 cell line at all ratios. There was no significant difference between control and drug-free SPNs in terms of cell viability ($p > 0.05$). On the other hand, curcumin/SPNs of all ratios showed significant inhibitory activity on cell growth. The viability of treated Saos2 cells with curcumin/SPNs was significantly lower than control group, drug-free SPNs, and free curcumin ($p < 0.05$). Quantification of anticancer activity also

Table 2 Comparison of IC50 value of free curcumin and curcumin–SPNs with various ratios

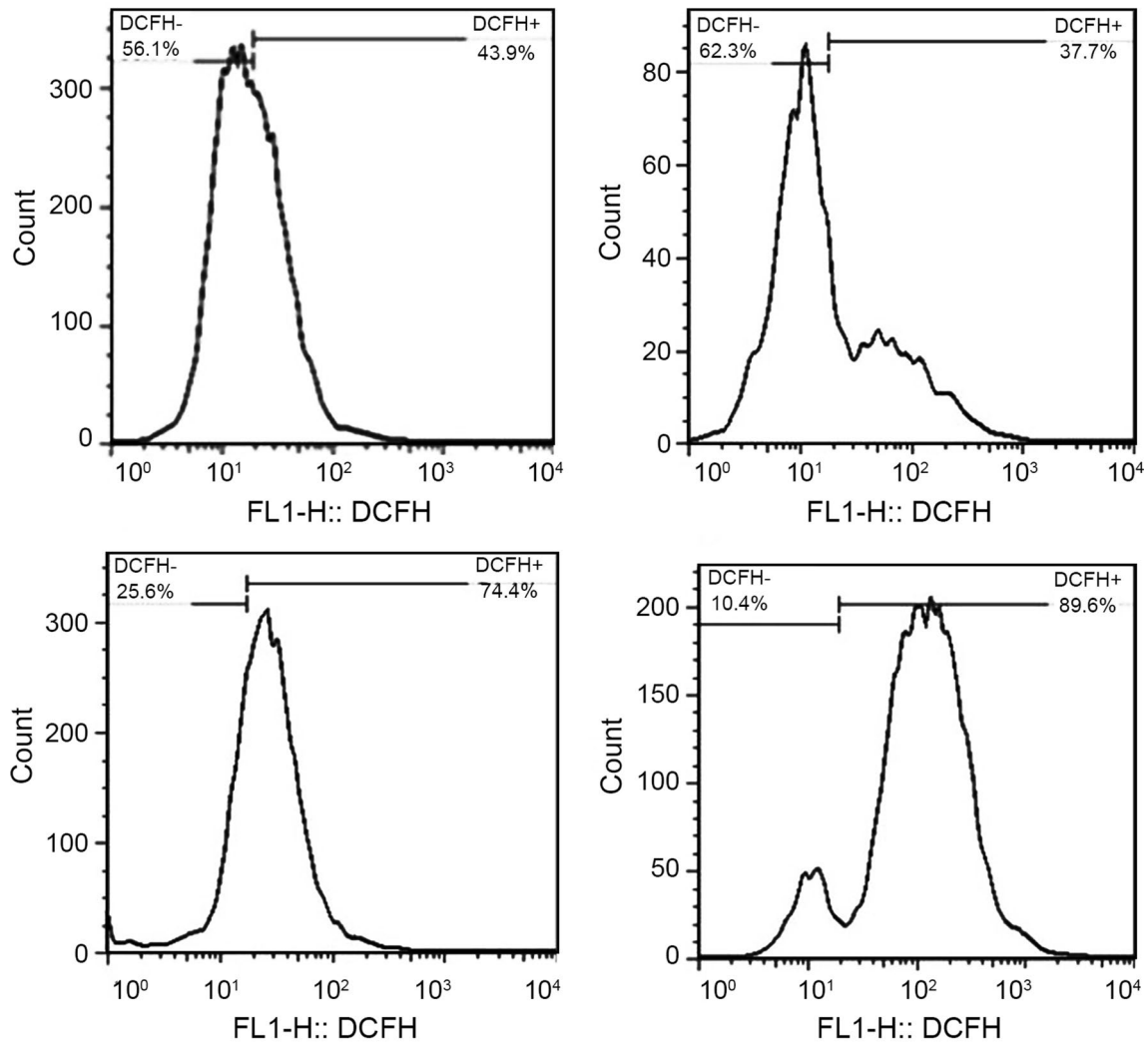| Samples	IC50 value (μg mL^{-1})	p value (free curcumin with curcumin–SPNs)
Free curcumin	156.8	0.025
Curcumin/SPNS		
1/10	65.9	
1/20	65.3	
1/30	64.8	
1/40	64.9	
p value (among curcumin–SPNs with different ratios)	0.981	

Fig. 5 Levels of intracellular reactive oxygen species (ROS) in the SAOS2 cell line. **A** Curcumin, **B** control, **C** curcumin/SPNs, **D** control
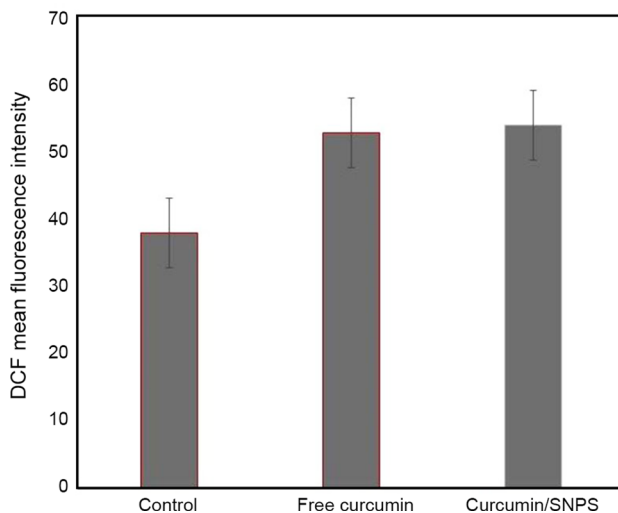
Fig. 6 Effects of drug treatment on intracellular reactive oxygen species (ROS) levels in in-vitro culture cell lines. DCF mean fluorescence intensity (MFI) was measured under basal (without 2′,7′-dichlorofluorescin (DCFH) treatment) and stimulated (DCFH+) conditions in SAOS2 that was subjected to drug treatment with the optimal dose of IC50 (Curcuminand Curcumin/SPNs). Data were as the mean ± SD. Data were obtained from at least three independent experiments. *$p < 0.05$ vs. control

showed that IC50 at all ratios of curcumin/SPNs was significantly lower than free curcumin ($p = 0.025$) (Table 2). There is no significant difference among IC50 values of curcumin/SPNs ratios ($p = 0.981$).

ROS assessment

According to Fig. 5, the mean intensity of emitted light from DCFH dye in the FL1-H channel was significantly increased to 168 in the treated SAOS2 cells compared to its control (36.3) for curcumin/SPNs. The mean intensity of emitted light from DCFH dye in the FL1-H channel was significantly increased to 44.5 in the treated Saos2 cells compared to its control (26.5) for free curcumin. Based on Fig. 6, the intracellular ROS levels significantly increased in an IC50 dose after 24 h of exposure to both free curcumin and curcumin/SPNs compared with controls ($p < 0.05$).

Discussion

Osteosarcoma is considered as bone cancer with different prevalence in adolescents and children (Ottaviani and Jaffe 2009). Similar to other cancer types, design and application of drug delivery systems can improve the treatment of Osteosarcoma (Li et al. 2016). Protein nanostructures, especially SPNs,

can be used as drug carrier for passive and active targeting of the cancer cells (Tang 2019). In this study, curcumin–SPNs were synthesized as potent drug for the treatment of osteosarcoma. Different ratios of SPNs/curcumin were applied for system design. Based on the results, the zeta potentials for drug-free SPNs and drug-loaded SPNs with different ratios of SPNs/curcumin are statistically similar with no significant difference. Literature review showed that this similarity of zeta potentials is due to low electrostatic interaction of curcumin with native charge of SPNs (Fukushima 1969; Malhotra and Coupland 2004; Phianmongkhol and Varley 2003). In FTIR spectra, nearly similar patterns were observed for free SPNs and drug-loaded SPNs. This situation showed that there is no free drug on the surface of SPNs. It also indicated the low leakage and fusion of encapsulated drug. According to our findings, the highest entrapment efficiency was observed in 1/10 of curcumin/SPNs. Also, entrapment efficiency decreased with increase of curcumin/SPNs ratio. Drug release profiles showed that there are similar patterns in the first hour for all the designed nanostructures. After 2 h, the decrease of drug release from nanostructures followed different slopes. The most concentrations of curcumin are loaded on a peripheral layer of SPNs. Therefore, high velocity of drug release in the first hours was due to this phenomenon. This situation was reported in various studies about soy proteins and other protein nanoparticles (Ezpeleta et al. 1996; Hu et al. 2008; Jithan et al. 2011; Patel et al. 2010; Yuan et al. 2020). After 2 h, the release of drug continued with mild slopes in all the designed nanoparticles. The drug release approximately reached 81–90% at the end of assessment time. Continuation of drug release in the second hour onwards was the result of curcumin transfer from the nucleus of nanoparticle to the surface (Luo et al. 2011). Anticancer activity assessment showed that the highest activity belonged to the ratio of 1/10 SPNs/curcumin. Similar studies proved that the reduction of nanoparticle size lead to its better penetration into the affected area as well as its escape from macrophage and other immune cells (Barua and Mitragotri 2014; Chenthamara et al. 2019; Desai et al. 2010). Therefore, among the examined nanoparticles in our study, the smallest nanoparticle had the highest anticancer activity due to better penetration into the cell. Previous studies have also shown that biomaterials delivery to special tissue has direct relationship with particles size (Ghafoorianfar et al. 2020). Reduction of SPs content for nanoparticle preparation can inhibit the hydrophobic chain-induced protein aggregation (Lagreca et al. 2020; Varanko et al. 2020). In smaller size of SPNs, curcumin can be better entrapped inside SPNs in comparison with larger nanoparticles. In our study, application of glutaraldehyde led to addition of amide bonds and prevention of particle deformation. On the other hand, SPNs with lower ratios of SPNs/curcumin has higher releasing rates due to smaller sizes and larger area/volume ratios. These smaller size and high area/volume ratios lead to better contact with the releasing medium. All

these conditions make SPNs, especially with smaller dimensions, which are effective drug systems for slow release. In our study, an increase of ROS production was observed in both treated cells with free curcumin and SPNs/curcumin. This increase was more evident in the SPNs/curcumin group than in free curcumin group. Based on literature review, this increase of ROS can be due to curcumin-induced destruction of mitochondrial function (Jena 2012). Findings of various studies have shown that excessive ROS generation after curcumin treatment is one of the most important mechanisms for inhibition of various tumor growth (Larasati et al. 2018; Nakamae et al. 2019; Wang et al. 2019, 2021, 2017). Our data showed similar results.

Conclusion

A slow release curcumin-containing soy protein nanoparticles was designed with potent anticancer activity and controlled release by controlling the particle size and SPNs/drug ratio. Our results showed that SPNs with smaller size and lower SPNs/drug can be used as a slow and controlled drug release system for anticancer agents. This designed nanoparticle can be used for delivery of other molecules and drugs besides curcumin. The synthesized SNPs can be used for delivery of chemotherapy drug to the target sites. This delivery can lead to enhancement of the therapeutic efficiency, reduction of drug use, as well as reduction of side effects.

Declarations

Conflict of interest The authors declare that they have no known competing financial interests.

Compliance with ethical standards The study was approved by Ethics Committee of Shahid Sadoughi University of Medical Sciences, Yazd, Iran (IR.SSU.MEDICINE.REC.1400.192).

References

Alemi A, Farrokhifar M, Zare-Zardini H, Karamallah MH (2018) A comparison between the anticancer activities of free paclitaxel and paclitaxel-loaded Niosome nanoparticles on human acute lymphoblastic leukemia cell line Nalm-6. Iran J Ped Hematol Oncol 8:153–160

Anitha A, Sreeranganathan M, Chennazhi KP, Lakshmanan VK, Jayakumar R (2014) In vitro combinatorial anticancer effects of 5-fluorouracil and curcumin loaded *N,O*-carboxymethyl chitosan nanoparticles toward colon cancer and in vivo pharmacokinetic studies. Eur J Pharma Biopharma 88:238–251

Barua S, Mitragotri S (2014) Challenges associated with penetration of nanoparticles across cell and tissue barriers: a review of current status and future prospects. Nano Today 9:223–243

Basnet P, Hussain H, Tho I, Skalko-Basnet N (2012) Liposomal delivery system enhances anti-inflammatory properties of curcumin. J Pharma Sci 101:598–609

Bhandari R, Gupta P, Dziubla T, Hilt JZ (2016) Single step synthesis, characterization and applications of curcumin functionalized iron oxide magnetic nanoparticles. Mater Sci Eng C 67:59–64

Chaurasia S, Chaubey P, Patel RR, Kumar N, Mishra B (2016) Curcumin-polymeric nanoparticles against colon-26 tumor-bearing mice: cytotoxicity, pharmacokinetic and anticancer efficacy studies. Drug Dev Ind Pharma 42:694–700

Chenthamara D, Subramaniam S, Ramakrishnan SG, Krishnaswamy S, Essa MM, Lin FH, Qoronfleh MW (2019) Therapeutic efficacy of nanoparticles and routes of administration. Biomater Res 23:20

Corre I, Verrecchia F, Crenn V, Redini F, Trichet V (2020) The osteosarcoma microenvironment: a complex but targetable ecosystem. Cells 9:976

Desai P, Patlolla RR, Singh M (2010) Interaction of nanoparticles and cell-penetrating peptides with skin for transdermal drug delivery. Mol Membr Biol 27:247–259

Di Natale C, Onesto V, Lagreca E, Vecchione R, Netti PA (2020) Tunable release of curcumin with an in silico-supported approach from mixtures of highly porous PLGA microparticles. Materials 1:1–12

Durfee RA, Mohammed M, Luu HH (2016) Review of osteosarcoma and current management. Rheuma Ther 3:221–243

Ege B, Yumrutas O, Ege M, Pehlivan M, Bozgeyik I (2020) Pharmacological properties and therapeutic potential of saffron (*Crocus sativus* L.) in osteosarcoma. 72:56–67

Elamin M, Al-Olayan E, Abdel-Gaber R, Yehia RS (2021) Antiproliferative and apoptosis induction activities of curcumin on Leishmania major. Revista Argen De Microbiol 53:240–247

Ezpeleta I, Irache JM, Stainmesse S, Chabenat C, Gueguen J, Popineau Y, Orecchioni AM (1996) Gliadin nanoparticles for the controlled release of all-trans-retinoic acid. Int J Pharm 131:191–200

Fukushima D (1969) Denaturation of soybean proteins by organic solvents. CER Chem 46:156

Ghafoorianfar S, Ghorani-Azam A, Mohajeri SA, Farzin D (2020) Efficiency of nanoparticles for treatment of ocular infections: systematic literature review. J Drug Deliv Sci Technol 1(57):101765

Giordano A, Tommonaro G (2019) Curcumin and cancer. Nutrients 11:2376

Hashimoto K, Nishimura S, Oka N, Akagi M (2020) Outcomes of comprehensive treatment for primary osteosarcoma. SAGE Open Med 8:2050312120923177–2050312120923177

Hewlings SJ, Kalman DS (2017) Curcumin: a review of its effects on human health. Foods (basel, Switzerland) 6:92

Hong S, Choi DW, Kim HN, Park CG, Lee W, Park HH (2020) Protein-based nanoparticles as drug delivery systems. Pharmaceutics 12:604

Hu B, Pan C, Sun Y, Hou Z, Ye H, Hu B, Zeng X (2008) Optimization of fabrication parameters to produce chitosan–tripolyphosphate nanoparticles for delivery of tea catechins. J Agric Food Chem 56:7451–7458

Jafari F, Javdansirat S, Sanaie S, Naseri A, Shamekh A, Rostamzadeh D, Dolati S (2020) Osteosarcoma: a comprehensive review of management and treatment strategies. Ann Diagn Pathol 49:151654

Jena N (2012) DNA damage by reactive species: mechanisms, mutation and repair. J Biosci 37:503–517

Jithan AV, Madhavi K, Madhavi M, Prabhakar K (2011) Preparation and characterization of albumin nanoparticles encapsulating curcumin intended for the treatment of breast cancer. Int J Pharma Invest 1:119

Kabir M, Rahman M, Akter R, Behl T, Kaushik D, Mittal V, Pandey P, Akhtar MF, Saleem A, Albadrani GM, Kamel M (2021) Potential role of curcumin and its nanoformulations to treat various types of cancers. Biomolecules 11:392

Kakkar V, Singh S, Singla D, Kaur IP (2011) Exploring solid lipid nanoparticles to enhance the oral bioavailability of curcumin. Mol Nutr Food Res 55:495–503

Kim S, Agca C, Agca Y (2013) Effects of various physical stress factors on mitochondrial function and reactive oxygen species in rat spermatozoa. Reprod Fert Dev 25:1051–1064

Lagreca E, Onesto V, Di Natale C, La Manna S, Netti PA, Vecchione R (2020) Recent advances in the formulation of PLGA microparticles for controlled drug delivery. Prog Biomat 9:153–174

Larasati YA, Yoneda-Kato N, Nakamae I, Yokoyama T, Meiyanto E, Kato JY (2018) Curcumin targets multiple enzymes involved in the ROS metabolic pathway to suppress tumor cell growth. Sci Rep 8(1):1–3

Li CJ, Liu XZ, Zhang L, Chen LB, Shi X, Wu SJ, Zhao JN (2016) Advances in bone-targeted drug delivery systems for neoadjuvant chemotherapy for osteosarcoma. Orthop Surg 8(2):105–110

Luo Y, Zhang B, Whent M, Yu LL, Wang Q (2011) Preparation and characterization of zein/chitosan complex for encapsulation of α-tocopherol, and its in vitro controlled release study. Colloids Surf B Biointerfaces 85(2):145–152

Malhotra A, Coupland JN (2004) The effect of surfactants on the solubility, zeta potential, and viscosity of soy protein isolates. Food Hydrocolloids 18(1):101–108

Mansouri K, Rasoulpoor S, Daneshkhah A, Abolfathi S, Salari N, Mohammadi M, Rasoulpoor S, Shabani S (2020) Clinical effects of curcumin in enhancing cancer therapy: a systematic review. BMC Cancer 20:791–791

Mohseni S, Aghayan M, Ghorani-Azam A, Behdani M, Asoodeh A (2014) Evaluation of antibacterial properties of barium zirconate titanate (BZT) nanoparticle. Braz J Microbiol 45:1393–1399

Mokarmat-Yazdi AA, Zare-Zardini H, Shayegh MR, Seifati SM (2021) Quranic and scientific study of the effect of germ of date seed on the P53 gene expression in breast cancer and normal human foreskin fibroblast cell lines. Quran Med 5:1–48

Mokarramat-Yazdi A, Soltaninejad H, Zare-Zardini H, Shishehbor F, Alemi A, Fesahat F, Sadeghian F (2020) Investigating the anticancer effect of a new drug originating from plant and animal: in vitro and in vivo study. J Adv Pharm Educ Res 10(S2):73

Mortezaee K, Salehi E, Mirtavoos-mahyari H, Motevaseli E, Najafi M, Farhood B, Rosengren RJ, Sahebkar A (2019) Mechanisms of apoptosis modulation by curcumin: Implications for cancer therapy. J Cell Physiol 234:12537–12550

Mpingirika EZ, El Hosseiny A, Bakheit SM, Arafeh R, Amleh A (2020) Potential anticancer activity of crude ethanol, ethyl acetate, and water extracts of ephedra foeminea on human osteosarcoma U2OS cell viability and migration. Biomed Res Int 2020:3837693–3837693

Nakamae I, Morimoto T, Shima H, Shionyu M, Fujiki H, Yoneda-Kato N, Yokoyama T, Kanaya S, Kakiuchi K, Shirai T, Meiyanto E (2019) Curcumin derivatives verify the essentiality of ROS upregulation in tumor suppression. Molecules 24:4067

Nambiar S, Osei E, Fleck A, Darko J, Mutsaers AJ, Wettig S (2018) Synthesis of curcumin-functionalized gold nanoparticles and cytotoxicity studies in human prostate cancer cell line. Appl Nanosci 8:347–357

Ntoutoume GM, Granet R, Mbakidi JP, Brégier F, Léger DY, Fidanzi-Dugas C, Lequart V, Joly N, Liagre B, Chaleix V, Sol V (2016) Development of curcumin–cyclodextrin/cellulose nanocrystals complexes: new anticancer drug delivery systems. Bioorg Med Chem Lett 26:941–945

Ottaviani G, Jaffe N (2009) The epidemiology of osteosarcoma. Cancer Treat Res 152:3–13

Patel A, Hu Y, Tiwari JK, Velikov KP (2010) Synthesis and characterisation of zein–curcumin colloidal particles. Soft Matter 6:6192–6199

Phianmongkhol A, Varley J (2003) ζ potential measurement for air bubbles in protein solutions. J Coll Interface Sci 260(2):332–338

Riahi-Zanjani B, Balali-Mood M, Asoodeh A, Es'haghi Z, Ghorani-Azam A (2019) Potential application of amino acids in analytical toxicology. Talanta 15(197):168–174

Semlali A, Contant C, Al-Otaibi B, Al-Jammaz I, Chandad F (2021) The curcumin analog (PAC) suppressed cell survival and induced apoptosis and autophagy in oral cancer cells. Sci Rep 11(1):1–15

Soltaninejad H, Zare-Zardini H, Hamidieh AA, Sobhan MR, Saeed-Banadaky SH, Amirkhani MA, Tolueinia B, Mehregan M, Mirakhor M (2020) Evaluating the toxicity and histological effects of Al$_2$O$_3$ nanoparticles on bone tissue in animal model: a case–control study. J Toxicol 2020:1–8

Soltaninejad H, Zare-Zardini H, Amirkhani MA, Mohammadzadeh M, Ghadiri-Anari A, Ordouei M, Alemi A, Ghorani-Azam A (2021) Effect of nanoalumina on sex hormones and fetuses in pregnant rats. JBRA Assist Reprod 26(2):241–246

Stanić Z (2017) Curcumin, a compound from natural sources, a true scientific challenge—a review. Plant Foods Hum Nutr 72:1–12

Tang CH (2019) Nanostructured soy proteins: Fabrication and applications as delivery systems for bioactives (a review). Food Hydrocolloids 91:92–116

Tefas LR, Sylvester B, Tomuta I, Sesarman A, Licarete E, Banciu M, Porfire A (2017) Development of antiproliferative long-circulating liposomes co-encapsulating doxorubicin and curcumin, through the use of a quality-by-design approach. Drug Des Dev Therapy 11:1605

Teng Z, Luo Y, Wang Q (2012) Nanoparticles synthesized from soy protein: preparation, characterization, and application for nutraceutical encapsulation. J Agric Food Chem 60:2712–2720

Varanko A, Saha S, Chilkoti A (2020) Recent trends in protein and peptide-based biomaterials for advanced drug delivery. Adv Drug Deliv Rev 156:133–187

Verma D, Gulati N, Kaul S, Mukherjee S, Nagaich U (2018) Protein based nanostructures for drug delivery. J Pharm 2018:9285854–9285854

Vetha BS, Kim EM, Oh PS, Kim SH, Lim ST, Sohn MH, Jeong HJ (2019) Curcumin encapsulated micellar nanoplatform for blue light emitting diode induced apoptosis as a new class of cancer therapy. Macromol Res 27(12):1179–1184

Wang L, Chen X, Du Z, Li G, Chen M, Chen X, Liang G, Chen T (2017) Curcumin suppresses gastric tumor cell growth via ROS-mediated DNA polymerase γ depletion disrupting cellular bioenergetics. J Exp Clin Cancer Res 36(1):1–4

Wang C, Song X, Shang M, Zou W, Zhang M, Wei H, Shao H (2019) Curcumin exerts cytotoxicity dependent on reactive oxygen species accumulation in non-small-cell lung cancer cells. Future Oncol 15(11):1243–1253

Wang S, Lu Y, Ouyang XK, Ling J (2020) Fabrication of soy protein isolate/cellulose nanocrystal composite nanoparticles for curcumin delivery. Int J Biol Macromol 165(Pt A):1468–1474

Wang H, Xu W, Sun J, Sui Z (2021) The novel curcumin derivative 1g induces mitochondrial and ER-stress-dependent apoptosis in colon cancer cells by induction of ROS production. Front Oncol 11:2233–2239

Weng W, Goel A (2020) Curcumin and colorectal cancer: an update and current perspective on this natural medicine. Semin Cancer Biol 80:73–86

Xin S, Wei G (2020) Prognostic factors in osteosarcoma: a study level meta-analysis and systematic review of current practice. J Bone Oncol 21:100281

Yuan H, Guo H, Luan X, He M, Li F, Burnett J, Truchan N, Sun D (2020) Albumin nanoparticle of paclitaxel (abraxane) decreases

while taxol increases breast cancer stem cells in treatment of triple negative breast cancer. Mol Pharm 17(7):2275–2286

Zare-Zardini H, Alemi A, Taheri-Kafrani A, Hosseini SA, Soltaninejad H, Hamidieh AA, Karamallah MH, Farrokhifar M, Farrokhifar M (2020) Assessment of a new ginsenoside Rh2 nanoniosomal formulation for enhanced antitumor efficacy on prostate cancer: an in vitro study. Drug Des Dev Ther 14:3315

Zhao X, Wu Q, Gong X, Liu J, Ma Y (2021) Osteosarcoma: a review of current and future therapeutic approaches. Biomed Eng Online 20(1):24–24